Title

Defined Culture of Human Embryonic Stem Cells and Xeno-Free Derivation of Retinal Pigmented Epithelial Cells on a Novel, Synthetic Substrate

Journal

Stem Cells Translational Medicine, 4(2)

ISSN

2157-6564

Authors

Pennington, Britney O
Clegg, Dennis O
Melkoumian, Zara K
et al.

Publication Date

2015-02-01

DOI

10.5966/sctm.2014-0179

Peer reviewed

STEM CELLS TRANSLATIONAL MEDICINE®

PROTOCOLS AND MANUFACTURING FOR CELL-BASED THERAPIES

Defined Culture of Human Embryonic Stem Cells and Xeno-Free Derivation of Retinal Pigmented Epithelial Cells on a Novel, Synthetic Substrate

BRITNEY O. PENNINGTON,[a] DENNIS O. CLEGG,[a,b] ZARA K. MELKOUMIAN,[c] SHERRY T. HIKITA[a,d]

Key Words. Human embryonic stem cells • Retinal pigmented epithelium • Synthemax II-SC substrate • Age-related macular degeneration • Parylene-C

[a]Center for Stem Cell Biology and Engineering, Neuroscience Research Institute, Biomolecular Science and Engineering Program and [b]Department of Molecular, Cellular and Developmental Biology, University of California, Santa Barbara, California, USA; [c]Corning Life Sciences Development, Corning Inc., Corning, New York, USA; [d]Asterias Biotherapeutics, Inc., Menlo Park, California, USA

Correspondence: Dennis O. Clegg, Ph.D., Neuroscience Research Institute, University of California, Santa Barbara, California 93106, USA. Telephone: 805-893-8490; E-Mail: clegg@lifesci.ucsb.edu

Received August 28, 2014; accepted for publication December 3, 2014; first published online in SCTM *EXPRESS* January 15, 2015.

1066-5099/2015/$20.00/0

http://dx.doi.org/10.5966/sctm.2014-0179

ABSTRACT

Age-related macular degeneration (AMD), a leading cause of blindness, is characterized by the death of the retinal pigmented epithelium (RPE), which is a monolayer posterior to the retina that supports the photoreceptors. Human embryonic stem cells (hESCs) can generate an unlimited source of RPE for cellular therapies, and clinical trials have been initiated. However, protocols for RPE derivation using defined conditions free of nonhuman derivatives (xeno-free) are preferred for clinical translation. This avoids exposing AMD patients to animal-derived products, which could incite an immune response. In this study, we investigated the maintenance of hESCs and their differentiation into RPE using Synthemax II-SC, which is a novel, synthetic animal-derived component-free, RGD peptide-containing copolymer compliant with good manufacturing practices designed for xeno-free stem cell culture. Cells on Synthemax II-SC were compared with cultures grown with xenogeneic and xeno-free control substrates. This report demonstrates that Synthemax II-SC supports long-term culture of H9 and H14 hESC lines and permits efficient differentiation of hESCs into functional RPE. Expression of RPE-specific markers was assessed by flow cytometry, quantitative polymerase chain reaction, and immunocytochemistry, and RPE function was determined by phagocytosis of rod outer segments and secretion of pigment epithelium-derived factor. Both hESCs and hESC-RPE maintained normal karyotypes after long-term culture on Synthemax II-SC. Furthermore, RPE generated on Synthemax II-SC are functional when seeded onto parylene-C scaffolds designed for clinical use. These experiments suggest that Synthemax II-SC is a suitable, defined substrate for hESC culture and the xeno-free derivation of RPE for cellular therapies. STEM CELLS TRANSLATIONAL MEDICINE *2015;4:165–177*

INTRODUCTION

Age-related macular degeneration (AMD) is the leading cause of blindness in people aged 65 and older in industrialized countries, accounting for 8.7% of the world's blind population, and it is projected that annual costs to the U.S. federal government will exceed $845 million by 2021 [1–3]. The early stages of this disease involve the dysfunction of the retinal pigmented epithelium (RPE). The RPE maintains the health of the photoreceptors through phagocytosis of shed outer segments, transporting and secreting ions and growth factors across the blood-retina barrier, isomerizing all-*trans*- to 11-*cis*-retinal to perpetuate the visual cycle, absorbing stray light, and limiting oxidation in the eye [4–6]. AMD manifests in two types. Exudative or "wet" AMD is characterized by choroidal neovascularization into the retina and can be mitigated by palliative intraocular injections of angiogenesis inhibitors such as Avastin, Lucentis, or EYLEA. However, 90% of AMD patients suffer from the "dry" form, which can lead to the geographic atrophy of the RPE and photoreceptors in the macular region of the retina [7]. As AMD progresses, the RPE degrade, causing the photoreceptors to deteriorate, which leads to an incapacitating loss of vision [8].

Currently, clinical studies are investigating the efficacy of transplanting RPE generated from human embryonic stem cells (hESC-RPE) and induced pluripotent stem cells (iPSC-RPE) as a means to preserve vision in AMD patients [9–11]. These pluripotent stem cell-derived RPE have already demonstrated visual rescue in an animal model of retinal degeneration, the Royal College of Surgeons (RCS) rat [12, 13]. One approach to deliver these cells is to inject a bolus suspension. Subjects receiving hESC-RPE suspensions in phase 1/2 clinical trials for AMD and Stargardt's macular dystrophy have not experienced adverse safety issues from the transplanted cells, whereas complications caused by surgery and immunosuppression have been observed. At the median 22-month follow-up, half of the patients have demonstrated visual improvement [9, 14]. However, diseased retinas among patients will display varying degrees of degeneration, and because

a suspension of RPE cells is extremely dissimilar to the endogenous organization, it is difficult to predict the efficacy of bolus injections as a therapy for the entire AMD population. Another approach undergoing clinical trials is to transplant a sheet consisting of autologous iPSC-RPE [11]. Sheets of iPSC-RPE express RPE markers and demonstrate function in vitro and in RCS rats. Furthermore, transplantation of autologous, nonhuman primate iPSC-RPE sheets does not invoke an immune response [11]. The structural integrity of the sheet and its proper orientation after surgery in human patients is currently under investigation. Alternatively, other groups are progressing to clinical trials using transplantable scaffolds, which provide a solid surface to promote a polarized RPE monolayer, enable site-specific delivery of the therapeutic cells, and confer support in a diseased environment [15, 16]. To this end, ultrathin parylene-C scaffolds have been engineered to provide a transplantable, semipermeable surface to support hESC-RPE therapeutic cells in the subretinal space [17, 18].

Parylene-C is a biostable polymer, and its deposition results in a conformal coat (i.e., a surface without pinholes) [19, 20]. It has a range of biomedical applications such as coating stents and pacemakers [20] and the circuitry of retinal prostheses [21, 22]. Established lithography techniques allow patterning of parylene-C into an array of ultrathin regions ($\sim$0.3 μm) that permit diffusion of biomolecules. These submicron regions are supported by a thicker meshwork of parylene-C ($\sim$6.0 μm) that provides mechanical support [23]. Parylene-C may be coated with full-length human vitronectin to allow attachment, polarization, and pigmentation of hESC-RPE [17].

Methods to culture and differentiate pluripotent stem cells into RPE often use xenogeneic mouse embryonic fibroblasts or Matrigel, a substrate derived from the Engelbreth-Holm-Swarm murine sarcoma [9, 11–13, 24]. These conditions present a possibility of exposing therapeutic cells to animal-derived immunogens, viruses, and other undefined components such as growth factors, collagenases, and plasminogen activators [25–27]. Recent efforts to derive hESC-RPE without using nonhuman animal products have cocultured hESCs with human foreskin fibroblasts and substrates comprised of full-length human proteins [28–30]. However, because of the natural variability among fibroblast cell lines or batches of purified proteins, synthetic substrates may be more desirable for consistent generation of clinical-grade therapies. Synthemax-R is a synthetic, animal-derived component-free (ACF) substrate designed for cell culture and is composed of a biologically active peptide derived from the human extracellular matrix (ECM) protein vitronectin that is covalently conjugated to the tissue culture vessel by an acrylate moiety [31]. ACF conditions do not use any animal-derived products, including human, and this distinguishes it from xeno-free conditions. Synthemax-R has been shown to support hESC and iPSC growth [31–37] and their differentiation into ocular cell types [32, 37, 38]. However, Synthemax-R is only available in limited styles of tissue culture plates, thus restricting its range of applications and its ability to scale up the manufacture of therapeutic cells. Synthemax-II SC Substrate, is a novel ACF, good manufacturing practice (GMP)-compliant peptide-copolymer that self-adsorbs onto tissue culture plastic or glass surfaces. This feature imparts versatility when scaling up production of therapeutic cells and facilitates a wider array of characterization assays. The Synthemax II-SC peptide includes the RGD-containing sequence from the human ECM protein vitronectin, KGGPQVT**RGD**VFTMP, which promotes adhesion in a variety of cells [31, 39, 40]. Synthemax II-SC differs from Synthemax-R in its coating chemistry and peptide density. Synthemax II-SC is a lyophilized powder that can be resuspended to a desired concentration, and its peptide noncovalently adsorbs to a surface. The covalently bound peptide on the Synthemax-R surface is more dense (8–12 pmol/mm^2) than the recommended coating density for Synthemax II-SC (5–10 pmol/mm^2) [31]. Synthemax II-SC is also less expensive; a six-well plate at the recommended coating density is less than half the cost of a Synthemax-R plate.

To date, Synthemax II-SC has been shown to support human iPSCs and human mesenchymal stem cells [41, 42]. Here we validate Synthemax II-SC as a viable substrate for the defined culture of hESCs and hESC-RPE. We have found that pluripotent H9 and H14 hESC lines can be maintained on Synthemax II-SC and retain a normal karyotype for more than 16 passages. These lines differentiate into hESC-RPE with a significantly higher yield of pigmented area than hESCs maintained on Synthemax-R Surface. Also, hESC-RPE cultured on Synthemax II-SC are similar to hESC-RPE derived on Matrigel and Synthemax-R with respect to gene expression and function. Furthermore, hESC-RPE derived on Synthemax II-SC retain RPE identity and function when seeded onto transplantable parylene-C scaffolds.

Materials and Methods

hESC Culture

Cultures of hESC lines H9 and H14 (WiCell Research Institute, Madison, WI, http://www.wicell.org) were maintained on Matrigel hESC-qualified matrix (catalog no. 354277; Corning Enterprises, Corning, NY, http://www.corning.com) in mTeSR1 (catalog no. 05850; StemCell Technologies, Vancouver, BC, Canada, http://www.stemcell.com). Stem cell colonies were manually passaged by hand every 4–7 days: differentiated regions were removed first, followed by a manual dissection of pluripotent colonies. To compare hESCs grown on Synthemax II-SC Substrate with other commercially available substrates, hESCs were passaged onto tissue culture-treated plates coated with Corning Matrigel, Corning Synthemax-R Surface (catalog nos. 3979, 3984, 3977XX1), and Synthemax II-SC Substrate (catalog no. 3536-XX1, lot no. DEV45-10; Corning Inc. Corning, NY, http://www.corning.com) and were serially passaged by manual dissection. Similar number and size of colonies were chosen for propagation on the three surfaces. hESCs between passages 40 and 49 were used for characterization. For differentiation into germ layers, hESCs on Synthemax II-SC were differentiated for 10 days in Dulbecco's Modified Eagle's Medium/F-12 + GlutaMAX I, 20% knockout serum replacement, 1$\times$ nonessential amino acids, and 0.1 mM β-mercaptoethanol (all reagents from Life Technologies, Carlsbad, CA, http://www.lifetech.com).

Differentiation, Enrichment, and Culture of hESC-RPE

A methods schematic is provided in supplemental online Figure 1. Pluripotent hESCs were spontaneously differentiated on the substrates of interest for 115 days in XVIVO10 medium (catalog no. 04-743Q; Lonza, Walkersville, MD, http://www.lonza.com) with Normocin (catalog no. ant-nr-1; Invivogen, San Diego, CA, http://www.invivogen.com/). Pigmented cells were enriched by treatment with TrypLE Select (catalog no. 12563-011; Gibco, Grand Island, NY, http://www.lifetechnologies.com), followed by manual removal of nonpigmented cells. The

remaining RPE were dissociated with TrypLE Select for 5 minutes at 37°C, passed through a 40-μm nylon cell strainer and seeded on the substrates of interest at 1.5×10^5 cells per cm^2. RPE cultures were maintained in XVIVO10 medium and passaged with TrypLE Select every 28 days for 3 months and seeded at 1.0×10^5 cells per cm^2 onto Matrigel, Synthemax-R, and Synthemax II-SC Substrate (catalog no. 3536-XX1, lot nos. 28512016, 14413006, 22413018). Cells at passage 2 day 28 were used for characterization. The "Matrigel," "Synthemax-R," and "Synthemax-II" designations describe the condition of hESCs propagated, differentiated, enriched, and passaged as RPE solely on the Matrigel, Synthemax-R, and Synthemax II-SC substrates, respectively. "Mg-SR" denotes the condition of undifferentiated hESCs grown and differentiated on Matrigel and then enriched and grown as RPE on Synthemax-R as described previously [18, 43].

Human Fetal RPE Culture

Human fetal RPE (fRPE) were a kind gift of Dean Bok (University of California Los Angeles) and Lincoln Johnson (Center for the Study of Macular Degeneration, University of California Santa Barbara). fRPE were maintained in Miller medium [44]: α-modification minimum essential medium (M4526; Sigma-Aldrich, St. Louis, MO, http://www.sigmaaldrich.com) supplemented with nonessential amino acids (catalog no. 11140-050; Gibco), GlutaMAX I (35050; Life Technologies), N1 supplement (N6530; Sigma-Aldrich), 1 ml of THT per 500 ml of medium (0.0065 μg/ml triiodothyronine; T5516, Sigma-Aldrich; 10 μg/ml hydrocortisone, Sigma-Aldrich; H0396, Sigma-Aldrich; 125 mg/ml taurine; T0625, Sigma-Aldrich) and heat-inactivated fetal bovine serum (15% for seeding fRPE, 5% for fRPE maintenance) (F-0500A; Atlas Biologicals, Fort Collins, CO, http://www.atlasbio.com/).

Synthemax II-SC Substrate Vessel Coating

Tissue culture vessels were coated with Synthemax II-SC according to the manufacturer's recommendations. Briefly, Synthemax II-SC powder was resuspended to 1 mg/ml in HyClone HyPure Cell Culture Grade Water (AWK21536) and either stored at 4°C for 1 month or further diluted 1:40 (0.025 mg/ml) to coat tissue culture vessels (CellBIND Surface, catalog no. 3335, Corning; cell culture plates and flasks, catalog nos. 3516, 3603, 430641, 431082, Corning Costar, Acton, MA, http://www.corning.com/lifesciences), Millicell-HA inserts (PIHA01250; Millipore, Billerica, MA, http://www.emdmillipore.com), and Lab-Tek Permanox Chamber Slides (catalog no. 177445; Thermo Fisher Scientific, Waltham, MA, http://www.thermofisher.com) at 5 μg/cm^2 for 2 hours at room temperature. The remaining Synthemax II-SC solution was aspirated, and the air-dried vessels were used immediately or stored at 4°C for up to 3 months.

Immunocytochemistry

Cells were rinsed with warm Dulbecco's phosphate-buffered saline (DPBS) (catalog no. 14190-144; Gibco) and fixed with an aqueous solution of 4.0% paraformaldehyde (catalog no. 15710; Electron Microscopy Sciences, Hatfield, PA, http://www.emsdiasum.com/microscopy) and 0.1 M sodium cacodylate buffer (catalog no. 11652; Electron Microscopy Sciences) for 5 minutes at 4°C. Fixed cells were blocked with 1% bovine serum albumin (BSA) (catalog no. 15260; Gibco), 1% goat serum (catalog no. G9023; Sigma-Aldrich), and 0.1% Triton X-100 (11332481001; Roche, Indianapolis, IN, http://www.roche.com) in phosphate-buffered saline (PBS) for 1 hour at 4°C. Primary antibodies diluted in block solution were applied overnight at 4°C (supplemental online Table 1). Cells were rinsed three times with PBS, and secondary antibodies were diluted 1:300 in block solution and applied for 30 minutes at 4°C (supplemental online Table 1). The cells were incubated with Hoechst nuclear stain (8 μg/ml, 33258; Sigma-Aldrich) for 5 minutes at room temperature in the dark and rinsed three times with PBS. Slides were mounted with Pro-Long Gold Antifade Reagent (catalog no. P36930; Life Technologies) and imaged with QCapture Pro software on Olympus IX71 or BX51 fluorescence microscopes (Olympus, Center Valley, PA, http://www.olympusamerica.com). Best1 localization was assessed with Fluoview software on an Olympus FV1000 confocal scanning microscope.

Quantitative Polymerase Chain Reaction

For RNA collection, whole wells of hESCs ready for passage were harvested from each substrate; differentiated regions were not removed prior to harvest. RNA was harvested using the RNeasy Plus kit (catalog no. 74136; Qiagen, Valencia, CA, http://www.qiagen.com) and converted to cDNA (iScript cDNA Synthesis kit; catalog no. 170-8891; Bio-Rad, Hercules, CA, http://www.bio-rad.com). For hESC-RPE, 1.5×10^5 cells were collected at passage 2 day 28 and processed with the Cells-to-Ct kit (catalog no. 4399002; Ambion, Austin, TX, http://www.ambion.com). Real-time quantitative polymerase chain reaction (qPCR) was completed with TaqMan Gene Expression Assays (catalog no. 4351372; Life Technologies; supplemental online Table 2) in TaqMan Gene Expression Master Mix (catalog no. 4369016; Life Technologies) using a Bio-Rad CFX96 real-time system. The data were analyzed with Bio-Rad CFX Manager software. Gene expression was normalized using the geometric mean of expression of the housekeeping genes SERF2, UBE2R2, and EIF2B2.

Flow Cytometry

Whole wells of hESCs ready for passage were harvested from each substrate; differentiated regions were not removed prior to harvest. hESCs were dissociated by 5- to 13-minute incubations in TrypLE Select at 37°C and diluted 1:5 in fresh medium. For hESC-RPE, 1×10^6 cells were collected at passage 2 day 28. For fixation, cells were centrifuged at 1,500 rpm for 3 minutes, washed in 0.5% BSA Fraction V (catalog no. 15260-037; Gibco) in PBS, and fixed in 4% paraformaldehyde in PBS for 20 minutes at room temperature in the dark. The cells were pelleted at 2,300 rpm for 3 minutes and permeabilized with 0.2% Triton X-100 (11332481001; Roche), 0.1% BSA Fraction V in PBS for 3 minutes at room temperature. Fixed cells were stored at 4°C in 0.5% BSA until stained.

Cells were stained with primary antibodies (supplemental online Table 1) diluted in 3% BSA in PBS for 30 minutes at 4°C (hESCs) or room temperature (RPE). Samples were stained with a secondary antibody (Alexa Fluor 488; A21202; Life Technologies) for 30 minutes at room temperature. Cells were rinsed with 0.5% BSA, and data were collected on a BD AccuriC6 Flow Cytometer with 10,000 gated events per sample. Gates were set to exclude 99.0% of the population stained with the isotype control of the primary antibody. The data were analyzed with FCS Express (De Novo Software, Glendale, CA, http://www.denovosoftware.com).

Karyotype

Cells were seeded in a T-25 flask (catalog no. 430168; Corning) that was coated with Matrigel or Synthemax II-SC Substrate and shipped in log phase overnight to Cell Line Genetics Inc. (Madison, WI, http://www.clgenetics.com/) for G-band karyotyping.

Pigmented Area Quantification

ImageJ was used to quantify pigmented area in the differentiated hESC cultures. Briefly, photographs of the differentiated hESC-RPE plates were converted to 8-bit images. Scale was set to 500 pixels: 17.3 mm for a six-well plate. The well area was selected, contrast-enhanced, background-subtracted, converted to binary, and analyzed for particle size (size 0.02–10 mm^2).

PEDF Enzyme-Linked Immunosorbent Assay

To compare secretion of pigment epithelium-derived factor (PEDF) hESC-RPE derived on different substrates were seeded onto Transwell Millicell-HA inserts (PIHA01250; Millipore) coated with 2.63 $\mu g/cm^2$ human vitronectin (354238; BD BioSciences, San Jose, CA, http://www.bdbiosciences.com) or Synthemax II-SC. The cells were maintained in 400 μl of XVIVO10 within the insert and 600 μl in the well. Apical and basal supernatants were collected on passage 2 day 30, 72 hours post-media change, snap-frozen in liquid nitrogen, and stored at $-80°C$. Supernatants from hESC-RPE on parylene-C membranes were collected 30 days after thaw/seed, 24 hours post media change. Supernatants were diluted 1:5,000; concentration of PEDF was determined with the PEDF enzyme-linked immunosorbent assay kit (catalog no. PED613-Human; Bioproducts MD, Middletown, MD, http://www.bioproductsmd.com/) according to the manufacturer's instructions. Optical density was measured at 450 nm.

ROS Phagocytosis

The Rod Outer Segment (ROS) phagocytosis assay was performed as previously described [45]. Briefly, hESC-RPE, human fRPE, and ARPE19 cells were seeded in quadruplicate onto gelatin, Synthemax II-SC, or human vitronectin-coated 96-well plates at 1×10^5 cells per cm^2 and maintained in Miller medium. Rod outer segments were isolated from fresh bovine retinas, labeled with fluorescein isothiocyanate (FluoReporter fluorescein isothiocyanate [FITC] protein labeling kit; catalog no. F6434; Life Technologies) and resuspended in 2.5% sucrose in Miller medium. Four weeks after plating, confluent cells were incubated with 1×10^6 labeled ROS, with or without 62.5μg/ml of the anti-$\alpha v\beta 5$ function blocking antibody (catalog no. ab24694; Abcam, Cambridge, U.K., http://www.abcam.com) or the isotype control (catalog no. ab18447; Abcam) for 5 hours at 37°C in 5% CO_2. Unbound ROS were removed with six rinses of warm 2.5% sucrose in PBS, and extracellular fluorescence was quenched with 0.4% trypan blue (catalog no. 25-900Cl; Corning) for 20 minutes at 37°C. Trypan blue was replaced with 40 μl of PBS-sucrose, and internalized fluorescence was imaged with an Olympus IX71. ImageJ software was used to calculate the internalized fluorescence intensity by pixel densitometry. Fluorescent signals from each condition were normalized to the ARPE19 signal.

hESC-RPE on Parylene-C

Mesh-supported submicron parylene-C scaffolds were manufactured as previously described, resulting in an array of ultrathin regions (~0.03 μm) supported by a thicker meshwork (~6 μm) [17]. These scaffolds were coated with human vitronectin in a 48-well plate. Briefly, scaffolds were placed in a 48 well plate with Teflon forceps, soaked in DPBS for 15 minutes, air-dried for 48 hours at room temperature, secured to the bottom of the plate with a cloning cylinder (CLS316610; Sigma-Aldrich), and coated with 250 μl of human vitronectin (10 μg/ml) for 2 hours at room temperature. Enriched hESC-RPE were cryopreserved and stored in liquid nitrogen (C. Presbey, M. Tsie, S. Hikita et al., manuscript in preparation). The cells were thawed and seeded onto vitronectin-coated parylene-C scaffolds at 1.5×10^5 cells per well and grown for 30 days in XVIVO10 medium without antibiotics.

Statistical Analysis

The two-tailed *t* test was used to determine the statistical significance of the differences between the amount of secreted PEDF by hESC-RPE on parylene-C membranes. The one-tailed *t* test was used to determine the statistical significance between the differences of internalized ROS fluorescence by hESC-RPE treated with $\alpha v\beta 5$ function blocking antibody versus isotype control. The one-tailed *t* test was also used to compare secretion of apical versus basal PEDF of hESC-RPE cultured on inserts. The level of *p* value that was considered significant has been denoted as ** for $p \leq .01$ and * for $p \leq .05$.

RESULTS

Synthemax II-SC Supports Long-Term Culture of H9 and H14 hESCs

Matrigel is one of the most widely used feeder-free substrates for hESC culture [24, 46]. Therefore, morphology and gene expression of hESCs cultured on Synthemax II-SC were compared with hESCs on Matrigel. Comparisons were also made to hESCs maintained on Synthemax-R to determine whether Synthemax II-SC is an acceptable alternative ACF substrate.

Overall, hESC colonies cultured on Synthemax II-SC exhibited morphology similar to hESCs grown on Matrigel, characterized by a homogenous layer of small, tightly packed cells, and a distinct colony border. Colonies on Synthemax II-SC qualitatively appeared larger than those grown on Synthemax-R but appeared to have thicker centers than the colonies grown on Matrigel. Colonies on Synthemax-R generally appeared smaller and thicker than those on the other two substrates and seemed to manifest more regions with differentiated morphology throughout the nine passages (Fig. 1A; supplemental online Fig. 2, arrowheads). Qualitatively, hESC colonies were easier to passage on Synthemax II-SC than Synthemax-R because colonies on the latter substrate remained small and developed compact, differentiated centers, rendering the efficient passaging of undifferentiated cells difficult.

Introducing hESCs to new culture conditions has been shown to elicit various fluctuations in morphology and an increase in differentiation while the cells adapt to the new environment [47, 48]. Previous studies have reported that hESCs undergo an adaption period once transferred to various feeder free substrates [49, 50]. H9 and H14 hESCs transitioning to Synthemax II-SC at passages 2 and 4, respectively, manifested dense differentiated areas harboring small regions devoid of cells within several colonies (supplemental online Fig. 2A, 2C, arrows). This extent of differentiation was not observed in other passages. However, it is known

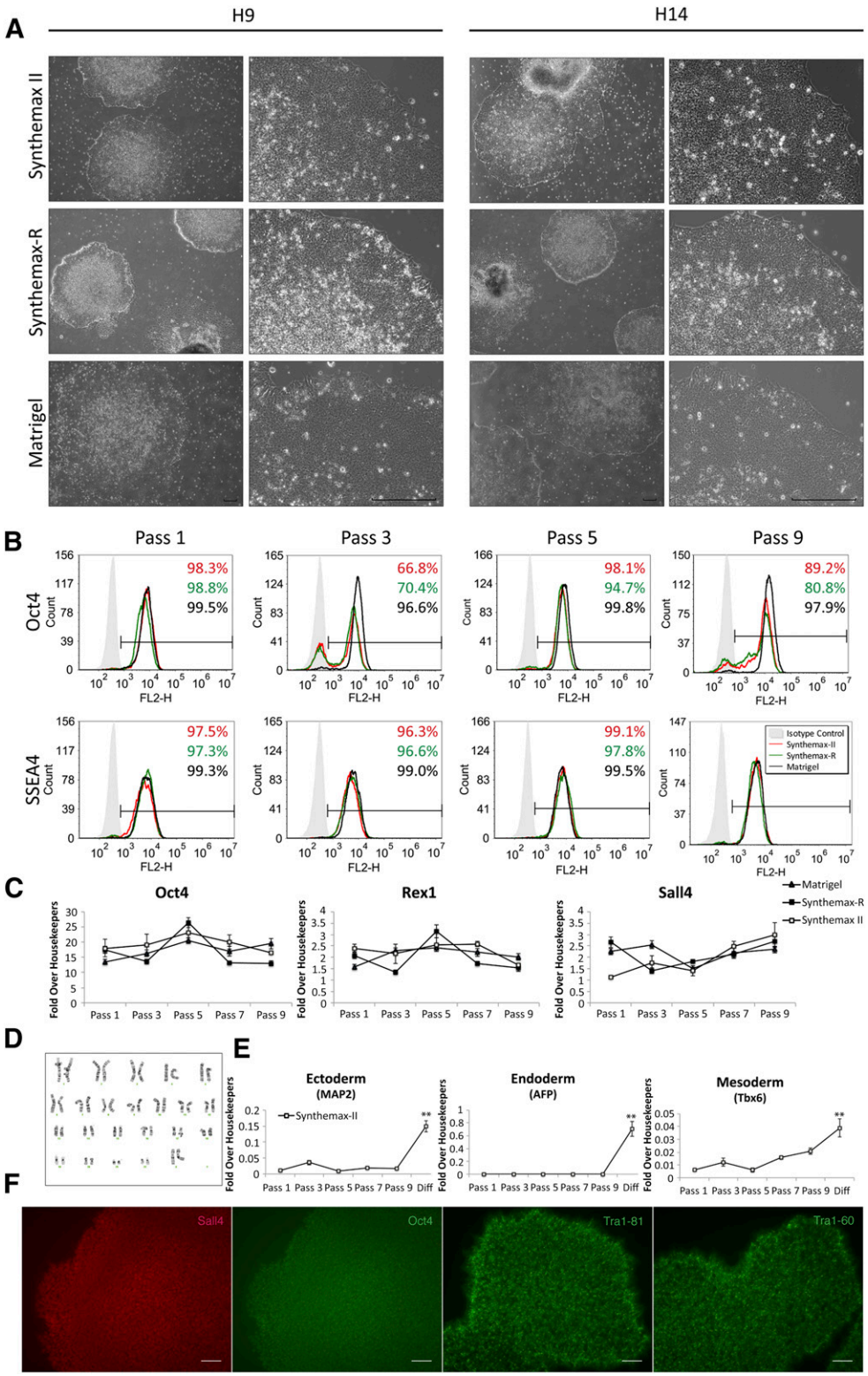

Figure 1. Characterization of human embryonic stem cells (hESCs) cultured on Synthemax II-SC, Synthemax-R, and Matrigel. **(A):** Representative phase-contrast micrographs of H9 and H14 hESC colony morphology after nine passages on the indicated substrate. Scale bars = 200 μm. **(B):** Representative flow cytometry histograms for pluripotency markers Oct4 and SSEA4 in H9 cultures grown on the indicated substrate at passages 1, 3, 5, and 9. **(C):** Relative expression of pluripotency genes in H9 cultures grown on Synthemax II-SC, Synthemax-R, and Matrigel at passages 1, 3, 5, and 9 as detected by quantitative polymerase chain reaction. **(D):** Normal karyotype of H9 hESCs maintained on Synthemax II-SC for 23 passages. **(E):** Relative gene expression of germ layer markers is significantly higher in H9 hESCs differentiated on Synthemax II-SC for 10 days compared with hESCs at earlier passages. **, $p < 0.01$, *t* test. **(F):** H9 hESCs on Synthemax II-SC stained for nuclear pluripotency transcription factors Oct4 and Sall4 and surface markers Tra-1-81 and Tra-1-60. Scale bars = 80 μm. Abbreviation: Diff, differentiation.

that healthy hESC cultures will experience a slight degree of differentiation in every passage, and some percentage of differentiation is expected [51]. In this regard, hESCs on Matrigel consistently demonstrated the least amount of differentiated morphology throughout nine passages. Because the original cultures for these experiments were previously adapted to Matrigel, the minimal differentiation observed in these cells is expected compared with the hESCs transitioning to a new substrate. Cultures of hESCs on Synthemax II-SC and Synthemax-R generally appeared slightly more differentiated than cells on Matrigel (supplemental online Fig. 2, arrowheads).

To investigate the percentage of cells expressing pluripotency markers Oct4 and SSEA4, flow cytometry was carried out on cultures at passages 1, 3, 5, and 9 (Fig. 1B; supplemental online Fig. 3A). Although hESCs on Matrigel consistently expressed both pluripotency markers, a decrease in Oct4 expression was observed on both xeno-free surfaces at some passages. Expression of SSEA4, however, was consistent on all three substrates throughout these passages. Additional markers of undifferentiated cells were examined by qPCR and immunocytochemistry. By passage 7, hESCs on Synthemax II-SC and Matrigel expressed similar levels of pluripotency-associated mRNAs (Fig. 1C; supplemental online Fig. 3B) and had similar colony morphologies. Throughout all passages, hESCs on Synthemax II-SC and Matrigel expressed the pluripotency surface antigens SSEA4, Tra-1-60, and Tra-1-81 along with nuclear hESC transcription factors Oct4 and Sall4 (Fig. 1B, 1F; supplemental online Fig. 3A, 3B). The H9 and H14 hESC lines continued to be subcultured for 23 and 16 passages, respectively, and each line maintained a normal karyotype (Fig. 1D; supplemental online Fig. 3D).

The differentiation potential of hESCs grown on Synthemax II-SC was investigated by culturing the cells in a differentiation medium for 10 days. These differentiated cells expressed markers from the three germ layers at significantly higher levels than the undifferentiated cultures ($p < .01$) (Fig. 1E; supplemental online Fig. 3C). Markers of ectoderm (MAP2 [microtubule-associated protein 2]) [34], mesoderm (Tbx6 [T-box protein 6]) [35], and endoderm (AFP [α-fetoprotein]) [52, 53] were detected. Taken together, these data demonstrate that Synthemax II-SC is a suitable, ACF substrate for the maintenance of hESCs that express canonical pluripotency markers and can differentiate into cells expressing markers of all three germ layers.

Synthemax II-SC Permits RPE Differentiation From hESCs

Because Synthemax II-SC was found to support the defined culture of hESCs, we next investigated whether this substrate also permitted efficient, xeno-free differentiation of hESCs into RPE. H9 and H14 hESC lines adapted to Matrigel, Synthemax-R, and Synthemax II-SC for seven passages were spontaneously differentiated into RPE by changing the growth medium to XVIVO10, a xeno-free formulation lacking basic fibroblast growth factor (Fig. 2). During this process, pigmented foci appeared after 4 weeks and continued to enlarge over the next few months. At 115 days postdifferentiation, the area of pigmentation on each substrate was quantified (Fig. 2). The lowest yield of pigmented area occurred on Synthemax-R. Surprisingly, Synthemax II-SC yielded significantly more pigmented area than Synthemax-R ($p < .01$). However, there was no difference in the amount of pigmented area produced on Matrigel and Synthemax II-SC. This suggests that Synthemax II-SC is an acceptable replacement for Matrigel in the xeno-free production of clinical-grade RPE from hESCs.

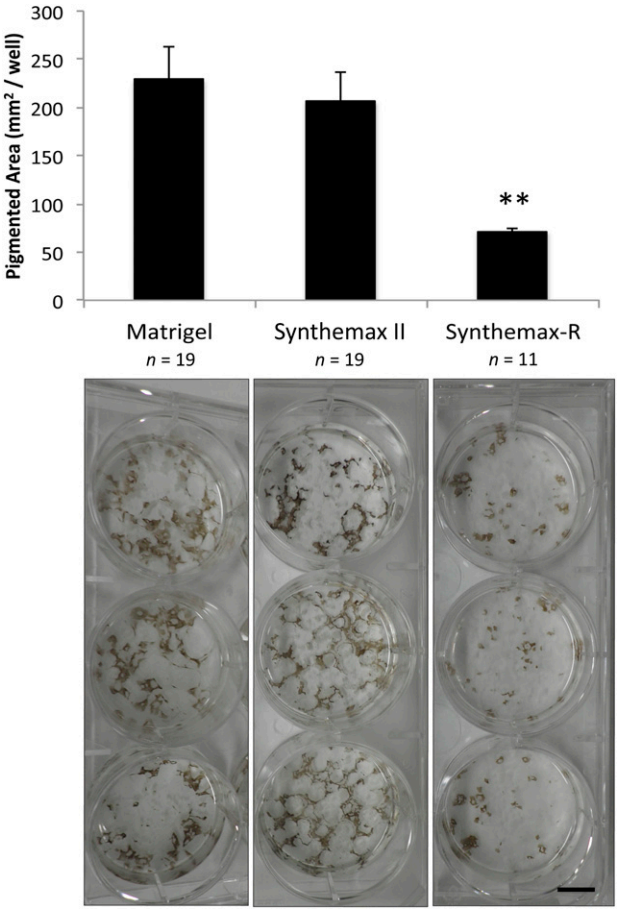

Figure 2. Spontaneous differentiation of retinal pigmented epithelia generated from human embryonic stem cells (hESC-RPE) on Matrigel and Synthemax II-SC yields significantly more pigmented area than hESC-RPE on Synthemax-R. Top: Pigmented area in individual wells was calculated with ImageJ software after 115 days of differentiation. Error bars denote standard deviation. **, $p < .01$, *t* test. Bottom: Three representative wells from a six-well plate of differentiated hESC-RPE seeded on each substrate are shown. Scale bar = 1 cm.

RPE Cultured on Synthemax II-SC Maintain RPE Identity

Pigmented regions produced by spontaneous differentiation (Fig. 2) were manually isolated from nonpigmented cells in a process termed "enrichment" (supplemental online Fig. 1). Protocols have been developed whereby hESCs are differentiated to RPE on Matrigel and then enriched onto Synthemax-R (Mg-SR method) [17, 18, 52–54]. To investigate whether Synthemax II-SC can entirely replace Matrigel for the growth of hESCs and their differentiation into RPE, we compared cultures maintained solely on Synthemax II-SC with those produced using the Mg-SR method. Synthemax II-SC hESC-RPE were also compared with cells produced solely on Synthemax-R or Matrigel.

After 30 days in culture, the hESC-RPE produced on Synthemax II-SC and Synthemax-R qualitatively appeared darker than those produced on Matrigel or by the Mg-SR method (Fig. 3A;

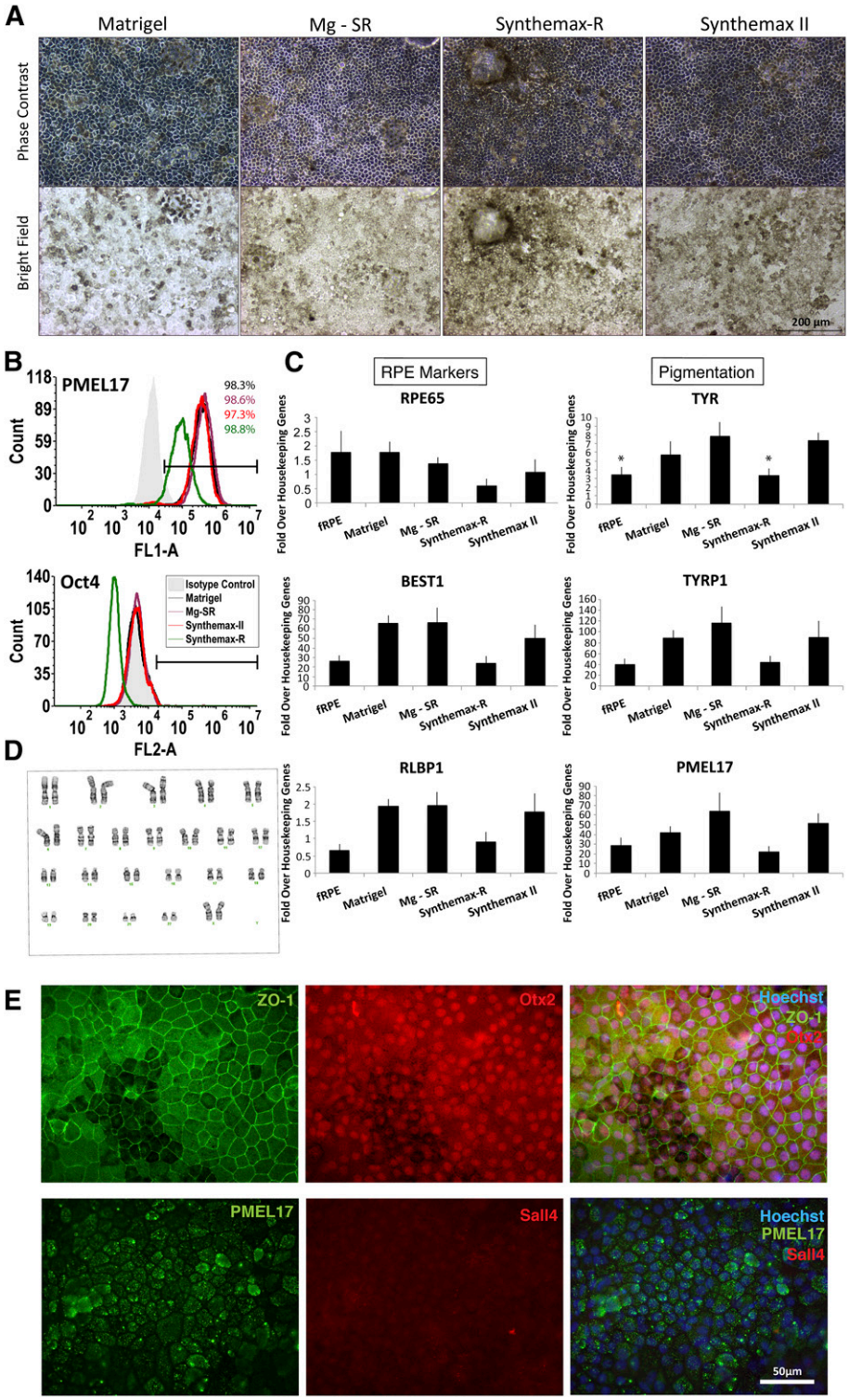

Figure 3. Characterization of RPE generated from human embryonic stem cells (hESC-RPE) derived on Synthemax II-SC. **(A):** Phase-contrast and bright-field images show the typical pigmentation and cobblestone morphology of H9 hESC-RPE cultured on different surfaces are shown. Scale bar = 200 μm. **(B):** Representative flow cytometry histograms are shown for the premelanosome pigmentation marker PMEL17 and the pluripotency marker Oct4 (not detected) in H9-RPE at passage 2 day 28 on the indicated substrate. **(C):** Expression of RPE marker genes in H9 hESC-RPE on the indicated substrates. fRPE served as a positive control (n = 3). $*$, $p < .05$, t test. **(D):** Normal karyotype of H9 hESC-RPE after spontaneous differentiation, enrichment, and three passages on Synthemax II-SC. **(E):** Epifluorescent images are shown of H9 hESC-RPE derived on Synthemax II-SC stained for the tight junction marker, ZO-1, RPE markers Otx2 and PMEL17, and the pluripotency marker Sall4 (not detected). Nuclei were detected using Hoechst (blue, merged right panels). Scale bar = 50 μm. Abbreviations: fRPE, fetal retinal pigmented epithelium; Mg-SR, condition of culturing and differentiating hESCs on Matrigel and then enriching and propagating the hESC-RPE on Synthemax-R; RPE, retinal pigmented epithelium.

supplemental online Fig. 4A). Expression of three pigmentation markers was investigated in each condition. Tyrosinase and tyrosinase-related protein-1 (Tyrp1) catalyze reactions in the melanogenesis pathway, and PMEL17 is a structural protein in premelanosomes. At passage 2 day 28, H9 hESC-RPE derived on Synthemax II-SC expressed Tyrp1 and PMEL17 similarly to those derived on the other substrates but expressed significantly more tyrosinase (Tyr) mRNA than RPE on Synthemax-R or fRPE controls (Fig. 3C). H14-derived RPE on Synthemax II-SC did not exhibit any difference in pigmentation marker expression compared with the other conditions (supplemental online Fig. 5A).

All conditions of each line displayed the typical cobblestone morphology of cultured RPE. A few lacunae were observed in a minority of hESC-RPE cultures on Synthemax II-SC at some passages (supplemental online Fig. 6A, 6B). These may be related to the efficiency of enrichment and the effects of paracrine signaling on tight junctions by non-RPE cells [55] or could be caused by miniscule bubbles that form during the Synthemax II-SC coating process that results in uneven peptide distribution. However, the hESC-RPE seemed to expand and fill the lacunae when cultured on Synthemax II-SC for 3 months or longer (supplemental online Fig. 6C).

The purity of the RPE population and efficiency of enrichment were measured at passage 2 day 28 by assessing the percentage of cells that express PMEL17, an essential structural protein for melanogenesis [56, 57]. All cultures were more than 95% positive for the protein PMEL17, and localization was confirmed by immunocytochemistry (Fig. 3B, 3E; supplemental online Fig. 4B, 4C). There was no significant difference in the expression of RPE65 and RLBP1 transcripts, which are involved in the visual cycle [6, 58], nor the RPE chloride channel, bestrophin-1 (BEST1) (Fig. 3C; supplemental online Fig. 5A). Furthermore, RPE produced on Synthemax II-SC expressed RPE marker proteins with proper localization. The RPE master transcription factor Otx2 [59, 60] was visualized in the nucleus and zonula occludens-1 (ZO-1) [6] immunoreactivity was observed at cell junctions, consistent with localization to tight junctions (Fig. 3E). BEST1 localized to the basal surface, which demonstrates that hESC-RPE on Synthemax II-SC achieve a polarized morphology (supplemental online Fig. 7).

One of the primary concerns regarding stem cell-derived therapies involves the potential of introducing tumorogenic, undifferentiated stem cells into patients [61]. Therefore, the expression of the pluripotency markers Oct4, Rex1, and Sall4 was assessed for all conditions of H9 and H14 hESC-RPE. All lines tested negative for these embryonic stem cell markers (Fig. 3B; supplemental online Figs. 4B, 4C, 5B, 5C). Also, the proliferative marker mKi67 could not be detected in any of the hESC-RPE derived under different conditions, which suggested that the cells are quiescent and have exited the cell cycle (supplemental online Fig. 5B, 5C). Furthermore, H9 and H14 hESCs that were grown, differentiated, enriched, and maintained as RPE for three passages on Synthemax II-SC retain a normal human karyotype (Fig. 3D; supplemental online Fig. 4D). These data demonstrate that hESC-RPE maintained in xeno-free conditions on Synthemax II-SC retain an RPE identity and are similar to RPE derived using the Mg-SR method.

RPE Derived on Synthemax II-SC Are Functional

One of the primary functions of RPE in the retina is to internalize the shed photoreceptor outer segments by phagocytosis [6, 62, 63]. The phagocytic function of hESC-RPE derived on Synthemax II-SC was compared with RPE generated on the other substrates. hESC-RPE on Synthemax II-SC internalized FITC-labeled ROS at levels similar to the other hESC-RPE (Fig. 4A; supplemental online Fig. 4E). In the first steps of ROS phagocytosis, integrin $\alpha v\beta 5$ physically binds the ROS, which activates focal adhesion kinase to stimulate receptor tyrosine kinase Mer to initiate ROS engulfment [62]. To test whether phagocytosis occurred via this pathway, function blocking antibodies to integrin $\alpha v\beta 5$ or an isotype control antibody were added with the ROS. Inhibiting $\alpha v\beta 5$ significantly reduced the amount of internalized ROS compared with the isotype control, indicating that hESC-RPE derived on Synthemax II-SC perform phagocytosis similarly to hESC-RPE derived on Matrigel, Synthemax-R, or Mg-SR ($p < .01$) (Fig. 4A; supplemental online Fig. 4E). Because vitronectin-coated scaffolds are being developed as cellular therapies for AMD [17], phagocytic function of hESC-RPE derived on Synthemax II-SC was analyzed on human vitronectin-coated plastic. hESC-RPE derived under defined, xeno-free culture conditions using Synthemax II-SC were capable of ROS phagocytic function when seeded on either vitronectin-coated surfaces or on Synthemax II-SC Substrate ($p < .01$) (Fig. 4B; supplemental online Fig. 3F).

In addition to phagocytosis, RPE are known to secrete growth factors that support the health of the neural retina and its structural integrity [6]. Among these is the apically secreted PEDF, which protects photoreceptors from ischemia and light damage [64, 65]. hESC-RPE derived on Synthemax II-SC secrete significantly more apical PEDF than basal PEDF when seeded on either xeno-free substrate of human vitronectin or Synthemax II-SC ($p < .01$). However, the amount of apical PEDF secreted by these cells is less than the apical PEDF secreted by hESC-RPE derived on Synthemax-R or by Mg-SR and fRPE (Fig. 4C). Taken together, these data demonstrate that hESC-RPE derived under xeno-free conditions on the synthetic Synthemax II-SC surface perform phagocytosis and apically secrete PEDF when seeded on defined substrates.

H9 hESC-RPE Derived on Synthemax II-SC Maintain RPE Identity and Function on Parylene-C Scaffolds

Vitronectin-coated mesh-supported submicron parylene-C scaffolds have been developed as transplantable surfaces to deliver hESC-RPE produced by the Mg-SR method into AMD patients [17, 18, 54]. To determine whether Synthemax II-SC can be used as a xeno-free alternative to the Mg-SR method to produce hESC-RPE, cells from these two conditions were cultured for 30 days on vitronectin-coated parylene-C scaffolds. No difference in initial attachment was observed, and hESC-RPE derived under both conditions grew to confluent monolayers with cobblestone morphology (Fig. 5A). Cells derived on Synthemax II-SC did not form lacunae when seeded onto vitronectin-coated parylene-C (n = 8 scafolds). Once again, darker pigmentation was observed in the hESC-RPE cultures generated on Synthemax II-SC by day 30 (Fig. 5A, 5B). However, there was no significant difference in the expression levels of genes associated with pigmentation as measured by qPCR (Fig. 5C). The mRNA encoding the melanocyte-specific Mitf-4 isoform (Mitf-M) was not detected, whereas variant 2 (Mitf-H), which is expressed during RPE development along with isoforms 1 and 7 (Mitf-A and Mitf-D), was observed (Fig. 5C) [66]. Although hESC-RPE derived on

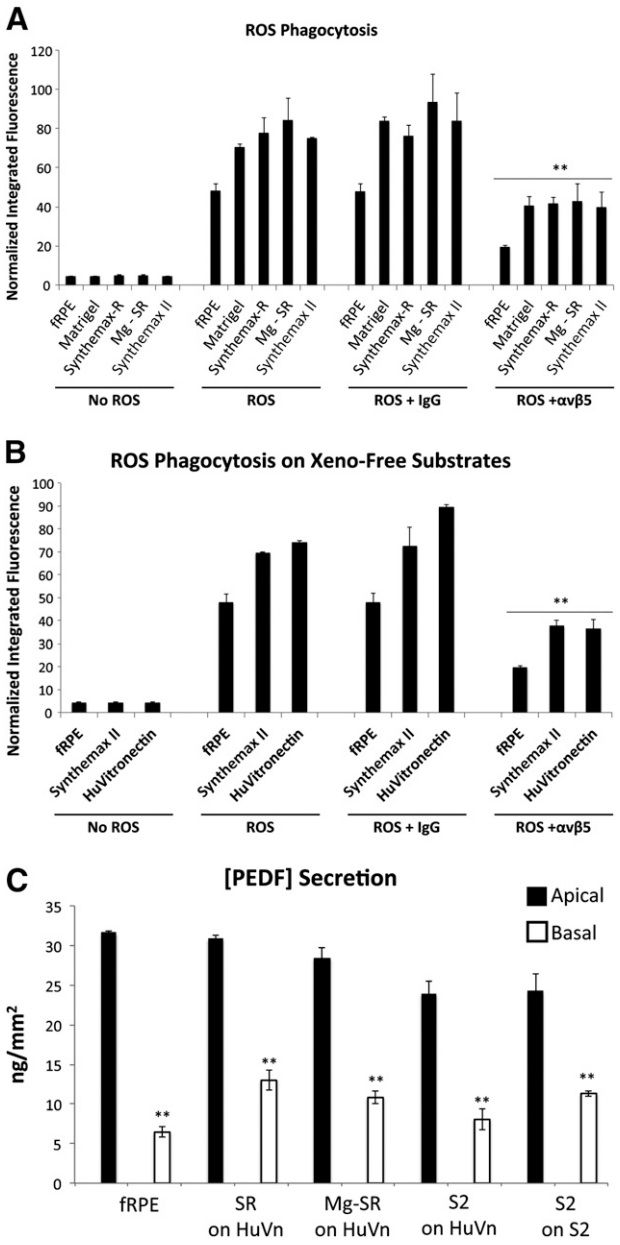

Figure 4. Functional characterization of H9 RPE generated from human embryonic stem cells (hESC-RPE) derived on Synthemax II-SC. **(A):** Phagocytosis of ROS by H9 hESC-RPE derived on Matrigel, Synthemax-R, Synthemax II-SC, or Mg-SR. A function-blocking antibody against $\alpha v\beta 5$ integrin, which is necessary for phagocytosis by RPE, significantly decreased internalization of ROS in all hESC-RPE when compared with the IgG isotype control. **, $p < .01$, *t* test. fRPE served as a positive control. **(B):** Phagocytosis of ROS by H9 hESC-RPE derived on Synthemax II-SC after seeding on the defined substrates Synthemax II-SC and human vitronectin. Phagocytic activity was significantly decreased with the function-blocking $\alpha v\beta 5$ antibody when compared with the IgG isotype control. **, $p < .01$, *t* test. **(C):** All conditions secrete PEDF significantly more on the apical surface compared with the basal side when seeded on surfaces coated with human vitronectin or Synthemax II-SC. **, $p < .01$, *t* test. hESC-RPE derived on Synthemax II-SC secrete less apical PEDF compared with fRPE and cells derived on Synthemax-R. Abbreviations: fRPE, fetal retinal pigmented epithelium; HuVn, human vitronectin; ROS, rod outer segment; S2, hESC-RPE derived on Synthemax II-SC; Mg-SR, hESCs grown and differentiated on Matrigel and then enriched as hESC-RPE on Synthemax-R; PEDF, pigment epithelium-derived factor; SR, hESC-RPE derived on Synthemax-R.

Synthemax II-SC expressed higher levels of RPE marker genes RPE65, Best1, and RLBP1 than the Mg-SR cells, this difference was not significant. The Synthemax II-SC hESC-RPE secreted ~18% less PEDF than hESC-RPE derived using the Mg-SR method (16 vs. 19.6 ng/mm^2) (Fig. 5D). However, both amounts are within the expected range of PEDF secretion by H9-derived RPE on parylene-C scaffolds (C. Hinman, D. Zhu, S. Hikita et al., manuscript in preparation). Taken together, these data suggest that Synthemax II-SC is a viable alternative to Matrigel for the xeno-free derivation and culture of hESC-RPE on parylene-C scaffolds.

Discussion

The advent of using pluripotent stem cell-derived therapies to treat human diseases necessitates good manufacturing practices and, preferably, defined culture conditions that do not use xenogeneic products [25]. However, some of the current methods used to produce hESC-RPE use Matrigel, a mixture of ECM proteins harvested from the Engelbreth-Holm-Swarm mouse sarcoma [17, 18, 54]. Coculturing therapeutic cells with xenogeneic derivatives may inadvertently introduce non-human viruses that could potentially inoculate the patient post-transplantation. Synthemax II-SC is a novel, ACF, GMP-compliant copolymer containing an RGD peptide. To date, it has been shown to support the growth of pluripotent human iPSCs as well as the large scale production of human mesenchymal stem cells [41, 42]. Here, we present the first characterization of hESC cultures and the xeno-free derivation of RPE using Synthemax II-SC. Furthermore, we have shown that hESC-RPE maintained on Synthemax II-SC express RPE markers and secrete PEDF when seeded onto transplantable parylene-C scaffolds. These data show that Matrigel can be entirely eliminated from the production of hESC-RPE and replaced with Synthemax II-SC.

Qualitatively, hESCs on Synthemax II-SC appeared larger than those grown on Synthemax-R. The observed restriction in colony size on the latter substrate may be due to the slightly higher density of peptide on the Synthemax-R Surface (8–12 pmol/mm^2) compared with the recommended coating density for Synthemax II-SC (5–10 pmol/mm^2) [31]. Consistent with this observation, a previous study has shown that human iPSC colonies on Synthemax-R were more compact than the Matrigel controls [36]. It is not uncommon to observe varying sizes of hESC colonies on various feeder-free substrates as demonstrated by a comparison of Matrigel, CELLstart, and vitronectin conducted by Yoon et al. [46].

The compact hESC colonies on Synthemax-R may also explain the significant decrease in the yield of pigmented area after spontaneous differentiation. For these experiments, pigmentation potential seemed to be augmented by a high confluence of hESCs and a low percentage of differentiation at the time of applying the XVIVO10 differentiation medium. Varying degrees of culture confluence have previously been implicated in determining the ultimate fate of differentiated stem cells [67, 68]. This may explain why the apparently smaller colonies on Synthemax-R gave a lower yield of pigmented area after spontaneous differentiation. Perhaps the lower peptide density of the Synthemax II-SC substrate permitted hESC colonies to expand more freely and achieve confluence faster than the cells on Synthemax-R. This could have augmented the yield of

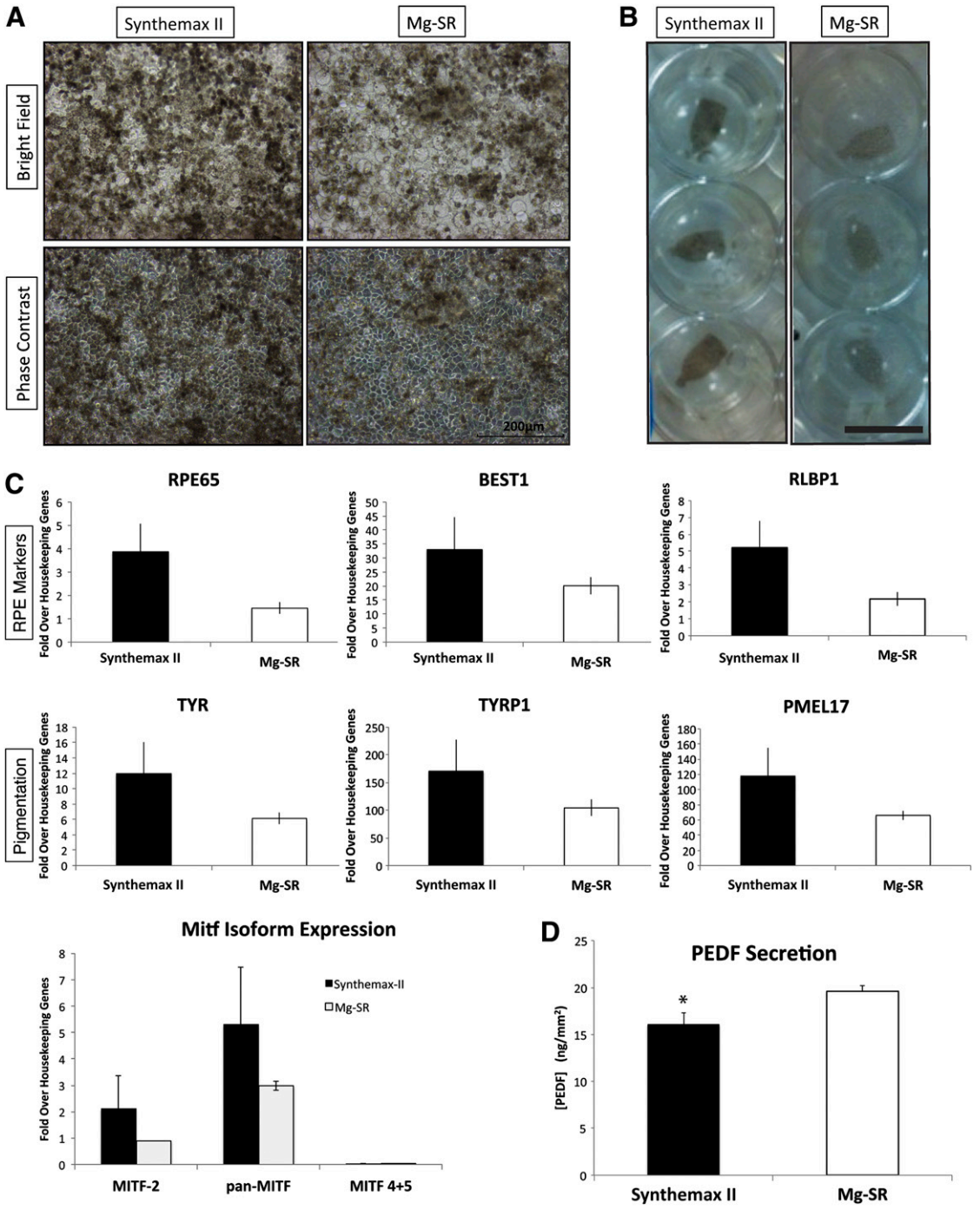

Figure 5. Characterization of H9 RPE generated from human embryonic stem cells (hESC-RPE) derived on Synthemax II-SC versus Mg-SR seeded onto parylene-C scaffolds. **(A):** Bright-field and phase-contrast images of H9 hESC-RPE cells grown for 30 days on parylene-C scaffolds. hESC-RPE were derived on Synthemax II-SC or by the Mg-SR method. Ultrathin regions of the membrane appear as an array of circles in the micrographs. Scale bar = 200 μm. **(B):** Bright-field images of three representative parylene-C scaffolds seeded with hESC-RPE in a 24-well plate (n = 8). Scale bar = 1 cm. Note darker pigmentation in the RPE derived on Synthemax II-SC. **(C):** Expression of RPE and pigmentation markers after 30 days on parylene-C scaffolds as detected by quantitative polymerase chain reaction (n = 3). **(D):** Quantification of PEDF protein secreted by hESC-RPE derived on Synthemax II-SC or by the Mg-SR method after 30 days on parylene-C scaffolds (n = 6; error is SEM). $*$, $p < .05$, t test. Abbreviations: Mg-SR, hESCs grown and differentiated on Matrigel and then enriched as hESC-RPE on Synthemax-R; PEDF, pigment epithelium-derived factor; RPE, retinal pigmented epithelium.

pigmented area after 115 days of spontaneous differentiation on Synthemax II-SC.

Flow cytometric analysis of hESCs at passages 1, 3, 5, and 9 revealed stable expression of the pluripotency-associated surface antigen SSEA4 [69] on all three substrates and a small subpopulation of cells negative for Oct4 on the synthetic surfaces at some passages. A previous study demonstrated that hESCs beginning to differentiate into an early neural lineage maintained high levels of

SSEA4 expression, whereas Oct4 was progressively downregulated [70]. The differentiated morphology seen in the cultures on the Synthemax surfaces could likely account for the small population of cells negative for Oct4 by flow cytometry. Despite the slightly smaller population positive for Oct4 at some passages, we conclude that Synthemax II-SC is a suitable, defined substrate for the maintenance of hESCs.

It is interesting that the H9-derived RPE on Synthemax II-SC express significantly higher Tyr mRNA than those on Synthemax-R, despite their similarities of darker pigmentation compared with the Matrigel cultures. RPE pigmentation performs a myriad of essential roles for vision such as protecting against harmful short-wavelength light, participating as an antioxidant to reduce oxidative damage, and even contributing to proper retinal structure during development [6, 71]. The macula is also reported to contain a higher concentration of pigment granules than the peripheral retina [72]. The discrepancy between the H9 Synthemax cultures could be due to differential rates of RPE maturation on the various substrates. During embryonic development of the optic cup, activation of the tyrosinase promoter initiates RPE maturation and melanogenesis [59, 71]. RPE then begin to produce melanosomes, which are specialized organelles for melanin synthesis. Tyrosinase, a heavily post-translationally modified enzyme, catalyzes the rate limiting step of melanin synthesis in developing melanosomes [57, 71, 73]. Pigment production in the RPE occurs during embryonic development, however, and no melanogenesis nor melanosome assembly is thought to occur after gestation [73]. RPE manifesting darker pigmentation may be more mature and could thus be starting to reduce the expression of melanogenesis genes while the proteins persist. Differential expression of gene transcripts and proteins for tyrosinase have been previously reported [74]. RPE pigmentation can vary considerably in vivo, however, and does not necessarily reflect on other functional capacities [12]. H14-derived RPE grown on the given substrates, however, did not have significant differences in the gene expression of pigmentation markers, so it will be interesting to determine if this trend in H9-derived RPE persists with further experimental repetitions.

hESC-RPE derived under xeno-free conditions with Synthemax II-SC demonstrated polarized secretory function and the ability to internalize ROS by phagocytosis. Regarding the secretory function of hESC-RPE, polarized secretion of PEDF testifies to the integrity of the tight junctions that separate the apical and basal environments, as well as to the maturity of the cells. H9 hESC-RPE on parylene-C scaffolds have been observed to secrete a range of apical PEDF concentrations between 11 and 20 ng/mm^2 of protein (C. Hinman, D. Zhu, S. Hikita et al., manuscript in preparation). When seeded on parylene-C scaffolds and culture inserts coated with human vitronectin, hESC-RPE derived on Synthemax II-SC secreted less PEDF than hESC-RPE derived by the Mg-SR method. However, the secreted amount of PEDF by the Synthemax II-SC cells on the scaffolds was still within the expected range. Whether these cells will increase the amount secreted PEDF as they mature in culture remains to be determined. It will also be interesting to investigate cell morphology and function when seeded on parylene-C scaffolds coated with Synthemax II-SC because the synthetic peptide contains the RGD binding site from vitronectin.

In summary, we have found that Matrigel can be replaced by the GMP-compliant substrate Synthemax II-SC for the culture of hESCs and the production of hESC-RPE. hESCs cultured on Synthemax II-SC express pluripotency markers and are capable of differentiation into cells expressing markers from the three germ layers. The yield of pigmented area on Synthemax II-SC after spontaneous differentiation of hESCs is significantly more than the yield on an alternative ACF substrate, Synthemax-R. hESC-RPE derived on Synthemax II-SC express RPE markers and internalize ROS by phagocytosis similarly to hESC-RPE derived on Matrigel and are also capable of PEDF secretion. Taken together, this work validates the use of a novel, ACF substrate for the defined culture of hESCs and the xeno-free production of hESC-RPE that can translate to stem cell-based therapies for human maladies such as AMD.

Conclusion

hESC-derived therapies are expected to be a powerful tool in regenerative medicine that requires defined, xeno-free culture conditions as the field moves forward. Here, we demonstrate that a novel synthetic substrate, Synthemax II-SC, supports pluripotent hESC cultures and promotes their efficient differentiation into functional RPE.

Acknowledgments

We thank the staff of the Center for Stem Cell Biology and Engineering, as well as the Laboratory for Stem Cell Biology and Engineering. This work was supported by the Richard & Katherine Gee Breaux Fellowship in Vision Research, the Garland Initiative for Vision, a grant-in-aid for research from the Scientific Research Society Sigma Xi, the Wynn-Gund Translational Research Acceleration Program, the University of California, Santa Barbara Institute for Collaborative Biotechnologies through Grant W911NF-09-0001 from the U.S. Army Research Office, and California Institute for Regenerative Medicine Grants DR1-01444, CL1-00521, TG2-01151, and FA1-00616 (to D.O.C.). Financial support from Fight for Sight is gratefully acknowledged. B.O.P. is a fellow of the California Institute for Regenerative Medicine. The content of the information does not necessarily reflect the position or the policy of the U.S. government, and no official endorsement should be inferred.

Author Contributions

B.O.P.: conception and design, collection and/or assembly of data, data analysis and interpretation, financial support, manuscript writing; D.O.C.: conception and design, financial support, data analysis and interpretation, final approval of manuscript; Z.K.M.: provision of study material, final approval of manuscript; S.T.H.: conception and design, data analysis and interpretation, final approval of the manuscript.

Disclosure of Potential Conflicts of Interest

D.O.C. has uncompensated employment, uncompensated intellectual property rights, and uncompensated ownership interest as co-owner of Regenerative Patch Technologies. Z.K.M. is a compensated employee of Corning Inc., which manufactures and sells Synthemax Surface product; a compensated inventor of Corning Inc., which is an assignee of the patent rights for Synthemax; and has been compensated with Corning stock options. S.T.H. has uncompensated intellectual property rights. The other author indicated no potential conflicts of interest.

REFERENCES

1 Rein DB, Zhang P, Wirth KE et al. The economic burden of major adult visual disorders in the United States. Arch Ophthalmol 2006;124: 1754–1760.

2 Wong WL, Su X, Li X et al. Global prevalence of age-related macular degeneration and disease burden projection for 2020 and 2040: A systematic review and meta-analysis. Lancet Glob Health 2014;2:e106–e116.

3 Khandhadia S, Cherry J, Lotery AJ. Age-related macular degeneration. Adv Exp Med Biol 2012;724:15–36.

4 Young RW, Bok D. Participation of the retinal pigment epithelium in the rod outer segment renewal process. J Cell Biol 1969;42: 392–403.

5 Miller SS, Edelman JL. Active ion transport pathways in the bovine retinal pigment epithelium. J Physiol 1990;424:283–300.

6 Strauss O. The retinal pigment epithelium in visual function. Physiol Rev 2005;85:845–881.

7 Carr A-JF, Smart MJK, Ramsden CM et al. Development of human embryonic stem cell therapies for age-related macular degeneration. Trends Neurosci 2013;36:385–395.

8 Hageman GS, Gehrs K, Johnson LV et al. Webvision: The Organization of the Retina and Visual System. Salt Lake City, UT: University of Utah Health Sciences Center, 1995.

9 Schwartz SD, Hubschman J-P, Heilwell G et al. Embryonic stem cell trials for macular degeneration: A preliminary report. Lancet 2012; 379:713–720.

10 Sipp D. Pilot clinical study into iPS cell therapy for eye disease starts in Japan | RIKEN. *rikenjp*. 2013. Available at http://www.riken.jp/en/pr/press/2013/20130730_1/. Accessed July 14, 2014.

11 Kamao H, Mandai M, Okamoto S et al. Characterization of human induced pluripotent stem cell-derived retinal pigment epithelium cell sheets aiming for clinical application. Stem Cell Reports 2014;2:205–218.

12 Lu B, Malcuit C, Wang S et al. Long-term safety and function of RPE from human embryonic stem cells in preclinical models of macular degeneration. STEM CELLS 2009;27: 2126–2135.

13 Carr A-J, Vugler AA, Hikita ST et al. Protective effects of human iPS-derived retinal pigment epithelium cell transplantation in the retinal dystrophic rat. PLoS ONE 2009;4:e8152.

14 Schwartz SD, Regillo CD, Lam BL et al. Human embryonic stem cell-derived retinal pigment epithelium in patients with age-related macular degeneration and Stargardt's macular dystrophy: Follow-up of two open-label phase 1/2 studies. Lancet 2014 [Epub ahead of print].

15 Binder S. Scaffolds for retinal pigment epithelium (RPE) replacement therapy. Br J Ophthalmol 2011;95:441–442.

16 Hynes SR, Lavik EB. A tissue-engineered approach towards retinal repair: Scaffolds for cell transplantation to the subretinal space. Graefes Arch Clin Exp Ophthalmol 2010;248: 763–778.

17 Lu B, Zhu D, Hinton D et al. Mesh-supported submicron parylene-C membranes for culturing retinal pigment epithelial cells. Biomed Microdevices 2012;14:659–667.

18 Hu Y, Liu L, Lu B et al. A novel approach for subretinal implantation of ultrathin substrates containing stem cell-derived retinal pigment epithelium monolayer. Ophthalmic Res 2012; 48:186–191.

19 Beach WF. Encyclopedia of Polymer Science and Technology. Hoboken, NJ: John Wiley & Sons, 2004.

20 Tan CP, Craighead HG. Surface engineering and patterning using parylene for biological applications. Materials (Basel) 2010;3: 1803–1832.

21 Li W, Rodger DC, Meng E et al. Wafer-level parylene packaging with integrated RF electronics for wireless retinal prostheses. J Microelectromech Syst 2010;19:735–742.

22 Menzel-Severing J, Laube T, Brockmann C et al. Implantation and explantation of an active epiretinal visual prosthesis: 2-year follow-up data from the EPIRET3 prospective clinical trial. Eye (Lond) 2012;26:501–509.

23 Lu B, Liu Z, Tai Y-C. Ultrathin parylene-C semipermeable membranes for biomedical applications. Micro Electro Mechanical Systems (MEMS), IEEE 24th International Conference, 2011:505–508.

24 Xu C, Inokuma MS, Denham J et al. Feeder-free growth of undifferentiated human embryonic stem cells. Nat Biotechnol 2001;19: 971–974.

25 O'Connor MD. The 3R principle: Advancing clinical application of human pluripotent stem cells. Stem Cell Res Ther 2013;4:21.

26 Vukicevic S, Kleinman HK, Luyten FP et al. Identification of multiple active growth factors in basement membrane Matrigel suggests caution in interpretation of cellular activity related to extracellular matrix components. Exp Cell Res 1992;202:1–8.

27 McGuire PG, Seeds NW. The interaction of plasminogen activator with a reconstituted basement membrane matrix and extracellular macromolecules produced by cultured epithelial cells. J Cell Biochem 1989;40:215–227.

28 Nakagawa M, Taniguchi Y, Senda S et al. A novel efficient feeder-free culture system for the derivation of human induced pluripotent stem cells. Sci Rep 2014;4:3594.

29 Vaajasaari H, Ilmarinen T, Juuti-Uusitalo K et al. Toward the defined and xeno-free differentiation of functional human pluripotent stem cell-derived retinal pigment epithelial cells. Mol Vis 2011;17:558–575.

30 Sorkio A, Hongisto H, Kaarniranta K et al. Structure and barrier properties of human embryonic stem cell-derived retinal pigment epithelial cells are affected by extracellular matrix protein coating. Tissue Eng Part A 2014;20:622–634.

31 Melkoumian Z, Weber JL, Weber DM et al. Synthetic peptide-acrylate surfaces for long-term self-renewal and cardiomyocyte differentiation of human embryonic stem cells. Nat Biotechnol 2010;28:606–610.

32 Tucker BA, Anfinson KR, Mullins RF et al. Use of a synthetic xeno-free culture substrate for induced pluripotent stem cell induction and retinal differentiation. STEM CELLS TRANSLATIONAL MEDICINE 2013;2:16–24.

33 Goh PA, Caxaria S, Casper C et al. A systematic evaluation of integration free reprogramming methods for deriving clinically relevant patient specific induced pluripotent stem (iPS) cells. PLoS ONE 2013;8:e81622.

34 Lin P-Y, Hung S-H, Yang Y-C et al. A synthetic peptide-acrylate surface for production of insulin-producing cells from human embryonic stem cells. Stem Cells Dev 2014;23: 372–379.

35 Li Y, Gautam A, Yang J et al. Differentiation of oligodendrocyte progenitor cells from human embryonic stem cells on vitronectin-derived synthetic peptide acrylate surface. Stem Cells Dev 2013;22:1497–1505.

36 Jin S, Yao H, Weber JL et al. Synthetic, xeno-free peptide surface for expansion and directed differentiation of human induced pluripotent stem cells. PLoS ONE 2012;7:e50880.

37 Maruotti J, Wahlin K, Gorrell D et al. A simple and scalable process for the differentiation of retinal pigment epithelium from human pluripotent stem cells. STEM CELLS TRANSLATIONAL MEDICINE 2013;2:341–354.

38 Baranov P, Regatieri C, Melo G et al. Synthetic peptide-acrylate surface for self-renewal of human retinal progenitor cells. Tissue Eng Part C Methods 2013;19:265–270.

39 Hayman EG, Pierschbacher MD, Ohgren Y et al. Serum spreading factor (vitronectin) is present at the cell surface and in tissues. Proc Natl Acad Sci USA 1983;80:4003–4007.

40 Ruoslahti E. RGD and other recognition sequences for integrins. Annu Rev Cell Dev Biol 1996;12:697–715.

41 Hervy M, Weber JL, Pecheul M et al. Long term expansion of bone marrow-derived hMSCs on novel synthetic microcarriers in xeno-free, defined conditions. PLoS ONE 2014;9:e92120.

42 Kelly J, Zhou J, Henry D et al. Feeder-Free Expansion of Human Induced Pluripotent Stem Cells (hiPSC) on Corning Synthemax-II SC Substrate Coated Surface in Defined Medium. *SnAPPShots*. 2012. Available at http://www.corning.com/lifesciences/surfaces/en/synthemax/technical_resources.aspx?linkidentifier=id&itemid=47257&menutitle=posters. Accessed July 15, 2014.

43 Buchholz DE, Hikita ST, Rowland TJ et al. Derivation of functional retinal pigmented epithelium from induced pluripotent stem cells. STEM CELLS 2009;27:2427–2434.

44 Maminishkis A, Miller SS. Experimental models for study of retinal pigment epithelial physiology and pathophysiology. J Vis Exp 2010;45:2032.

45 Buchholz DE, Pennington BO, Croze RH et al. Rapid and efficient directed differentiation of human pluripotent stem cells into retinal pigmented epithelium. STEM CELLS TRANSLATIONAL MEDICINE 2013;2:384–393.

46 Yoon T-M, Chang B, Kim H-T et al. Human embryonic stem cells (hESCs) cultured under distinctive feeder-free culture conditions display global gene expression patterns similar to hESCs from feeder-dependent culture conditions. Stem Cell Rev 2010;6:425–437.

47 Bigdeli N, Andersson M, Strehl R et al. Adaptation of human embryonic stem cells to feeder-free and matrix-free culture conditions directly on plastic surfaces. J Biotechnol 2008;133:146–153.

48 Stover AE, Schwartz PH. Adaptation of human pluripotent stem cells to feeder-free conditions in chemically defined medium with enzymatic single-cell passaging. Methods Mol Biol 2011;767:137–146.

49 Tompkins JD, Hall C, Chen VC-Y et al. Epigenetic stability, adaptability, and reversibility in human embryonic stem cells. Proc Natl Acad Sci USA 2012;109:12544–12549.

50 Ramos-Mejia V, Bueno C, Roldan M et al. The adaptation of human embryonic stem cells to different feeder-free culture conditions is accompanied by a mitochondrial response. Stem Cells Dev 2012;21:1145–1155.

51 Perkel J. Tricks for Human Embryonic Stem Cells. The Scientist.com. 2005. Available at http://www.the-scientist.com/?articles.view/articleNo/16566/title/Tricks-For-Human-Embryonic-Stem-Cells/. Accessed July 16, 2014.

52 Kwon GS, Fraser ST, Eakin GS et al. Tg (Afp-GFP) expression marks primitive and definitive endoderm lineages during mouse development. Dev Dyn 2006;235:2549–2558.

53 Dziadek M, Adamson E. Localization and synthesis of alphafoetoprotein in post-implantation mouse embryos. J Embryol Exp Morphol 1978;43:289–313.

54 Diniz B, Thomas P, Thomas B et al. Subretinal implantation of retinal pigment epithelial cells derived from human embryonic stem cells: Improved survival when implanted as a monolayer. Invest Ophthalmol Vis Sci 2013;54:5087–5096.

55 Lagunoff D, Rickard A. Mast cell granule heparin proteoglycan induces lacunae in confluent endothelial cell monolayers. Am J Pathol 1999;154:1591–1600.

56 Kobayashi T, Urabe K, Orlow SJ et al. The Pmel 17/silver locus protein: Characterization and investigation of its melanogenic function. J Biol Chem 1994;269:29198–29205.

57 Wasmeier C, Hume AN, Bolasco G et al. Melanosomes at a glance. J Cell Sci 2008;121:3995–3999.

58 Saari JC, Nawrot M, Kennedy BN et al. Visual cycle impairment in cellular retinaldehyde binding protein (CRALBP) knockout mice results in delayed dark adaptation. Neuron 2001;29:739–748.

59 Clegg DO, Buchholz D, Hikita S et al. Retinal pigment epithelial cells: Development in vivo and derivation from human embryonic stem cells in vitro for treatment of age-related macular degeneration. Stem Cell Research and Therapeutics. New York, NY: Springer Science + Business Media, 2008:1–24.

60 Meyer JS, Shearer RL, Capowski EE et al. Modeling early retinal development with human embryonic and induced pluripotent stem cells. Proc Natl Acad Sci USA 2009;106:16698–16703.

61 Tung P-Y, Knoepfler PS. Epigenetic mechanisms of tumorigenicity manifesting in stem cells. Oncogene 2014 [Epub ahead of print].

62 Finnemann SC. Focal adhesion kinase signaling promotes phagocytosis of integrin-bound photoreceptors. EMBO J 2003;22:4143–4154.

63 D'Cruz PMP, Yasumura D, Weir J et al. Mutation of the receptor tyrosine kinase gene Mertk in the retinal dystrophic RCS rat. Hum Mol Genet 2000;9:645–651.

64 Cao W, Tombran-Tink J, Elias R et al. In vivo protection of photoreceptors from light damage by pigment epithelium-derived factor. Invest Ophthalmol Vis Sci 2001;42:1646–1652.

65 Ogata N, Wang L, Jo N et al. Pigment epithelium derived factor as a neuroprotective agent against ischemic retinal injury. Curr Eye Res 2001;22:245–252.

66 Bharti K, Liu W, Csermely T et al. Alternative promoter use in eye development: The complex role and regulation of the transcription factor MITF. Development 2008;135:1169–1178.

67 Chambers SM, Fasano CA, Papapetrou EP et al. Highly efficient neural conversion of human ES and iPS cells by dual inhibition of SMAD signaling. Nat Biotechnol 2009;27:275–280.

68 Lane A, Philip LR, Ruban L et al. Engineering efficient retinal pigment epithelium differentiation from human pluripotent stem cells. STEM CELLS TRANSLATIONAL MEDICINE 2014;3:1295–1304.

69 Adewumi O, Aflatoonian B, Ahrlund-Richter L et al. Characterization of human embryonic stem cell lines by the International Stem Cell Initiative. Nat Biotechnol 2007;25:803–816.

70 Noisa P, Ramasamy TS, Lamont FR et al. Identification and characterisation of the early differentiating cells in neural differentiation of human embryonic stem cells. PLoS ONE 2012;7:e37129.

71 Jeffery G. The retinal pigment epithelium as a developmental regulator of the neural retina. Eye (Lond) 1998;12:499–503.

72 Boulton M, Dayhaw-Barker P. The role of the retinal pigment epithelium: Topographical variation and ageing changes. Eye (Lond) 2001;15:384–389.

73 Sarna T. Properties and function of the ocular melanin: A photobiophysical view. J Photochem Photobiol B 1992;12:215–258.

74 Hashimoto Y, Ito Y, Kato T et al. Expression profiles of melanogenesis-related genes and proteins in acquired melanocytic nevus. J Cutan Pathol 2006;33:207–215.

See www.StemCellsTM.com for supporting information available online.

